Supporting Information

Cr^{3+}-free near-infrared persistent luminescence material $LiGaO_2:Fe^{3+}$: optical properties, afterglow mechanism and potential bioimaging

Zhihao Zhou,[a] Xiaodong Yi,[b] Puxian Xiong,[a] Xingyi Xu,[a] Zhijun Ma,[a] and Mingying Peng[a*]

[a.] *The China-Germany Research Center for Photonic Materials and Devices, The State Key Laboratory of Luminescent Materials and Devices, and Guangdong Provincial Key Laboratory of Fiber Laser Materials and Applied Techniques, The School of Materials Science and Engineering and The School of Physics, South China University of Technology, Guangzhou 510640, P. R. China.*

[b.] *CAS Key Laboratory of Design and Assembly of Functional Nanostructures, and Fujian Key Laboratory of Nanomaterials, Fujian Institute of Research on the Structure of Matter, Chinese Academy of Sciences, Fuzhou, Fujian 350002, P. R. China.*

[*]Corresponding author:

E-mail: pengmingying@scut.edu.cn

Table S1. Ion radius and electronegativity of Li^+, Ga^{3+}, and Fe^{3+} ions.

Ion	Coordination number	r (Å)	$r_{difference}$ (%)*	Electronegativity (eV)
Li^+	4	0.59	16.95%	0.98
Ga^{3+}	4	0.47	4.25%	1.81
Fe^{3+}	4	0.49	—	1.83

*$r_{difference} = (r_{solute}-r_{solvent})/r_{solvent} \times 100\%$[1]

Table S1 shows the comparison of the ion radius and electronegativity of Li^+, Ga^{3+}, and Fe^{3+} ions. The ion radius (in the case of four coordination) and electronegativity of Fe^{3+} and Ga^{3+} are very close. According to the Hume-Rother rule, the ionic radius difference between Fe^{3+} (0.49 Å) and Ga^{3+} (0.47 Å) ions is 4.25%, which is much lower than the threshold value 15% of good solubility (whereas, the difference between Fe^{3+} and Li^+ is 16.95%). Besides, the valence states of Fe^{3+} and Ga^{3+} ions are the same. According to these theoretical analyses, the Ga^{3+} sites are supposed to be occupied by the doped Fe^{3+} ions in theory.

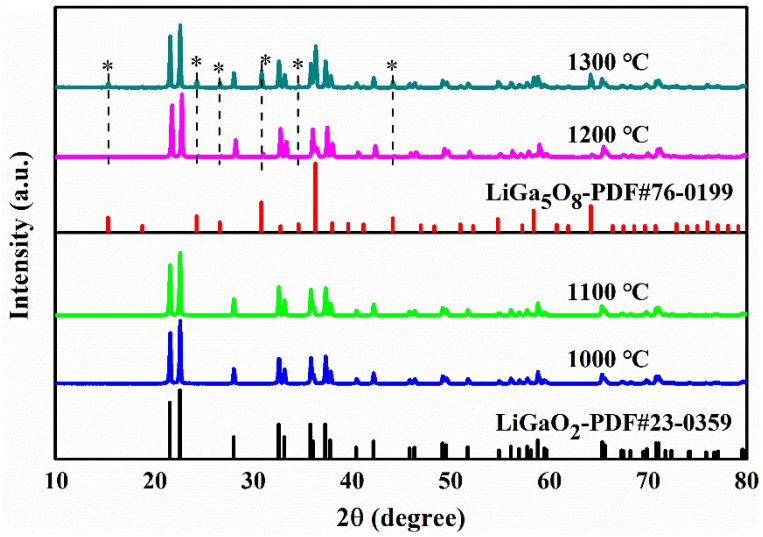

Fig. S1 XRD patterns of $LiGaO_2$:0.25%Fe^{3+} phosphors prepared at different temperatures (* represents the $LiGa_5O_8$ impurity phase).

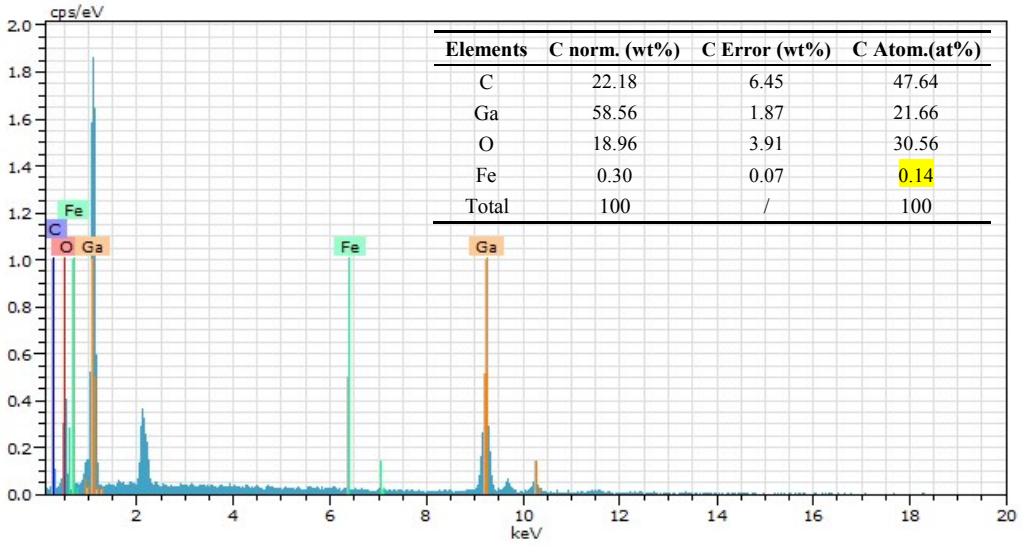

Elements	C norm. (wt%)	C Error (wt%)	C Atom.(at%)
C	22.18	6.45	47.64
Ga	58.56	1.87	21.66
O	18.96	3.91	30.56
Fe	0.30	0.07	0.14
Total	100	/	100

Fig. S2 Energy dispersive X-ray spectra (EDS) of $LiGaO_2$:0.25%Fe^{3+} sample, showing the elements of Ga, Fe, and O in the phosphor. The absence of Li element in EDX is due to Li atomic mass is too small to generate a reliable X-ray signal for detection. The inset shows the chemical compositions of the phosphor determined by EDS, revealing 0.14% of Fe^{3+} in the sample, which is close to the theoretical value.

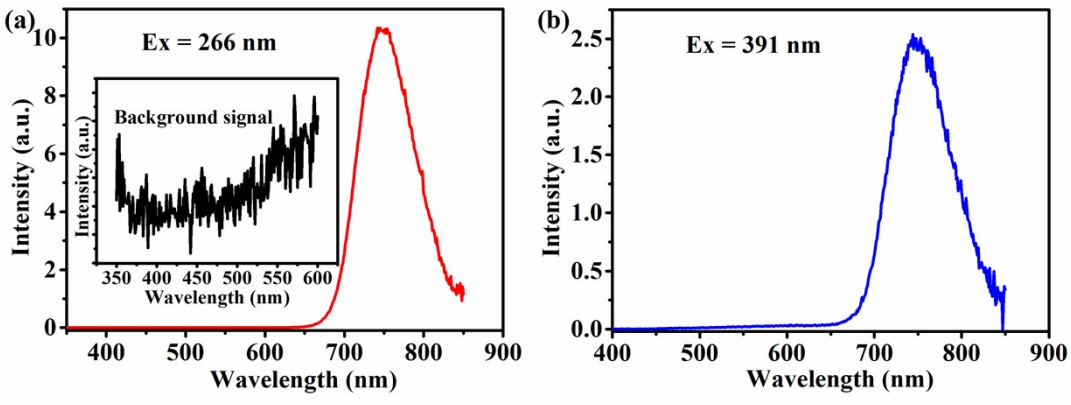

Fig. S3 Photoluminescence (PL) spectra (range from 350 nm to 850 nm) of $LiGaO_2$:0.25%Fe^{3+} sample under (a) 266 nm and (b) 391 nm excitation. The inset shows the test data from 350 nm to 600 nm, and no visible PL emission was detected.

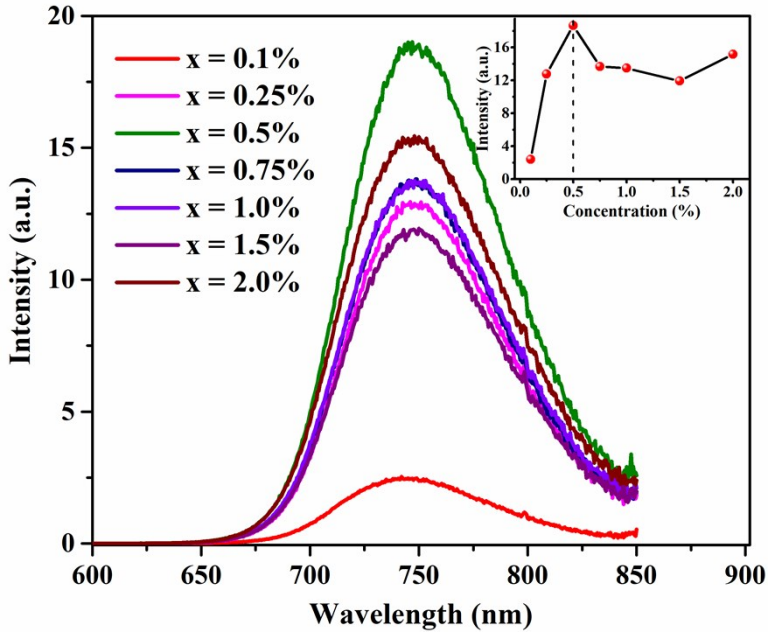

Fig. S4 Photoluminescence (PL) spectra of $LiGaO_2$:xFe^{3+} (x = 0.1-2.0%) samples under 266 nm excitation. The inset shows the relationship between the integral PL intensity and the Fe^{3+} doping concentration.

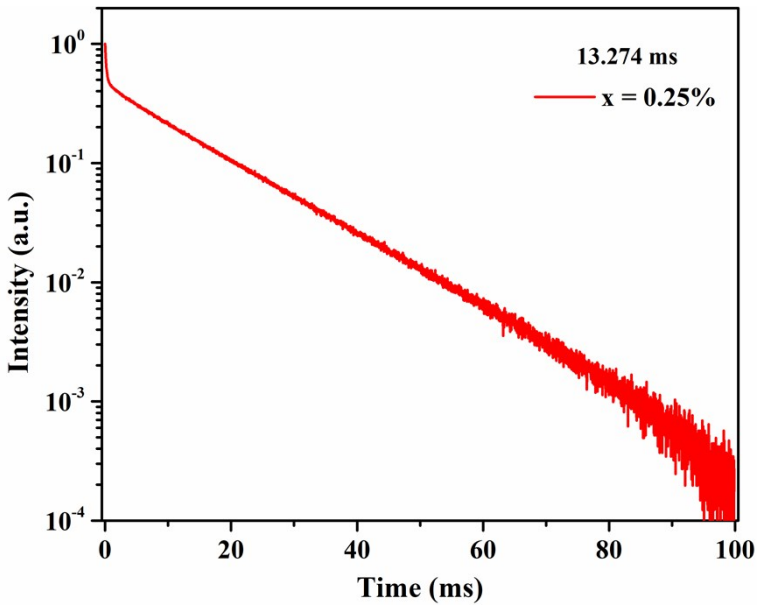

Fig. S5 PL decay curve of $LiGaO_2$:0.25%Fe^{3+} sample monitored at 748 nm under 266 nm excitation. The effective PL lifetime was determined by:[2, 3]

$$\tau_{eff} = \frac{1}{I_{max}} \int_0^\infty I(t)dt$$

where *I(t)* denotes the PL intensity as a function of time *t*, and I_{max} represents the maximum PL intensity.

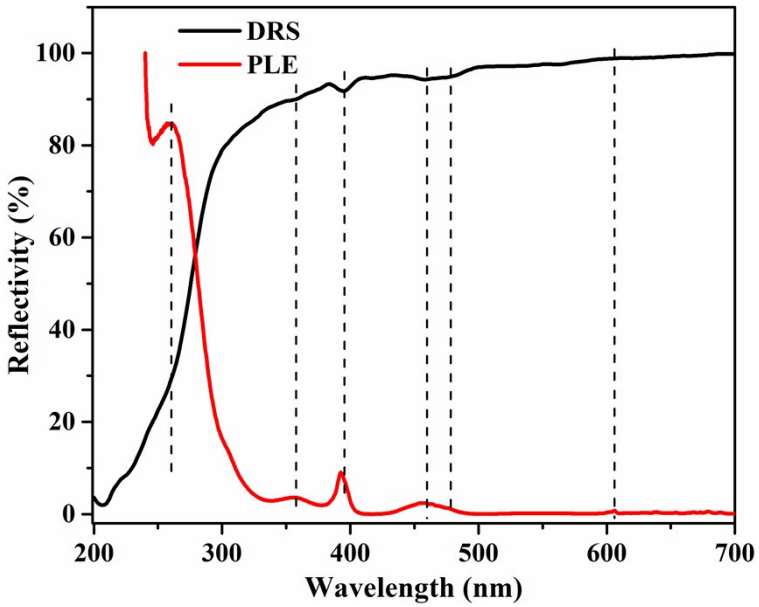

Fig. S6 The diffuse reflection spectra (DRS) of $LiGaO_2$:0.25%Fe^{3+}, and the corresponding photoluminescence excitation (PLE) spectrum monitored at 748 nm.

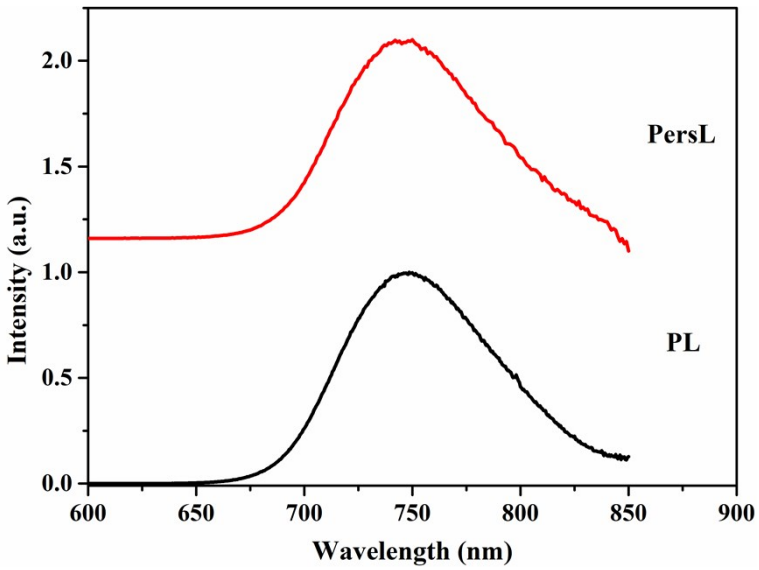

Fig. S7 The normalized PL and persistent luminescence (PersL) spectra of $LiGaO_2$:0.25%Fe^{3+}.

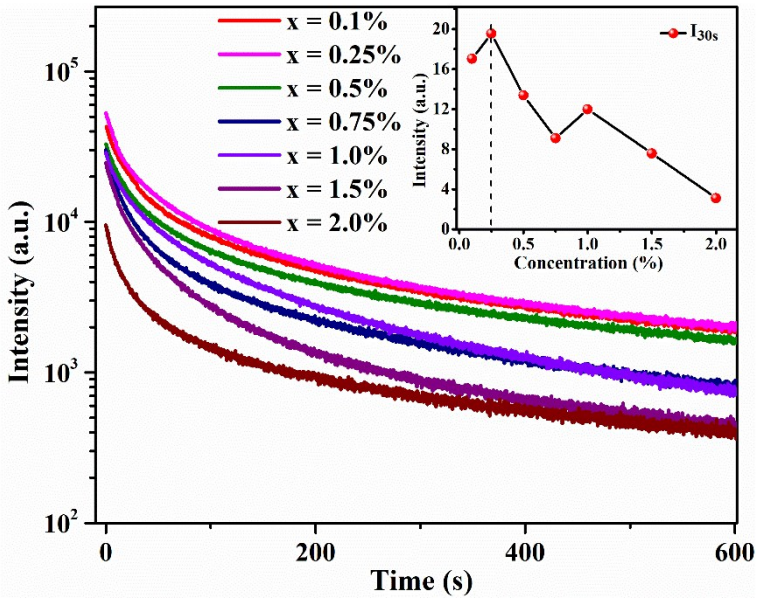

Fig. S8 PersL decay curves of the as-prepared $LiGaO_2$:xFe^{3+} (x = 0.1-2.0%) samples (recorded for 600 s). The inset shows the PersL intensities at different Fe^{3+} doping concentration, the PersL decay intensity values recorded at 30 s were used as the reference points.

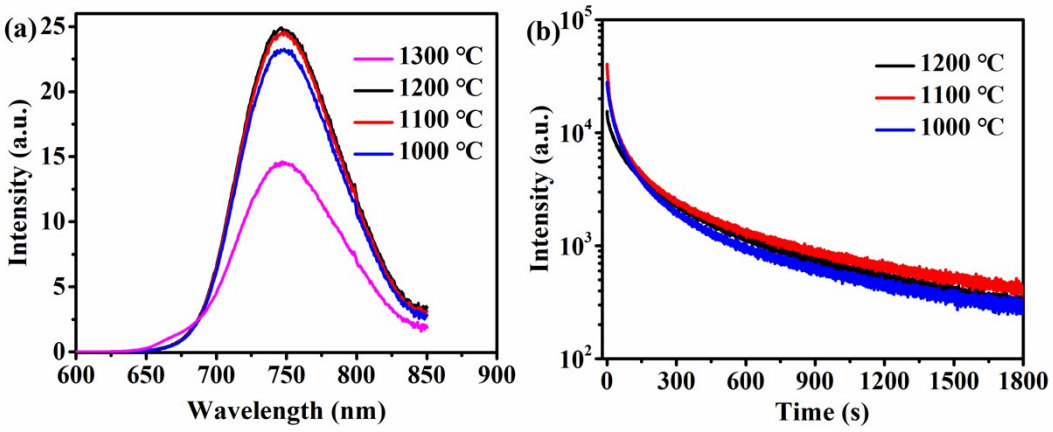

Fig. S9 (a) PL spectra and (b) PersL decay curves of $LiGaO_2$:0.25%Fe^{3+} phosphors prepared at different temperatures.

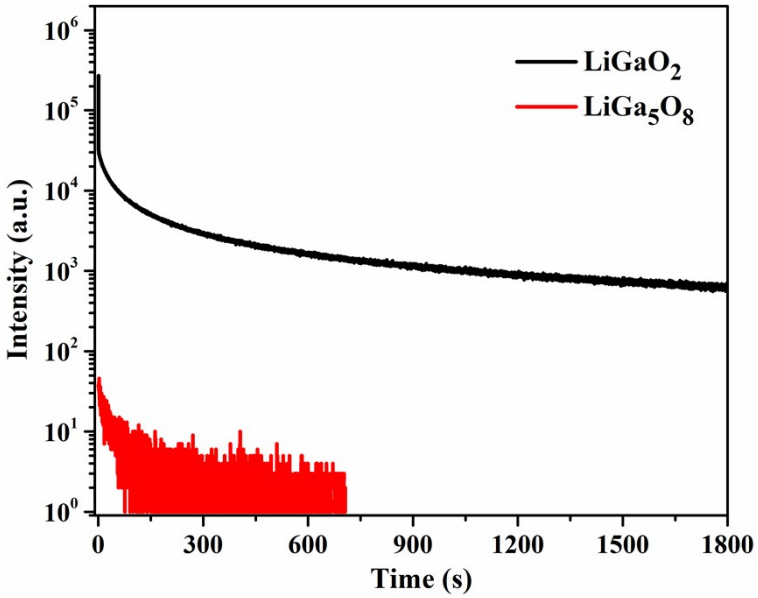

Fig. S10 PersL decay curves of Fe^{3+}-doped $LiGaO_2$ and $LiGa_5O_8$ phosphors, respectively. The Fe^{3+}-doped $LiGa_5O_8$ sample shows the faint PersL signal, indicating that the $LiGa_5O_8$ host is not suitable for the Fe^{3+} to produce NIR PersL.

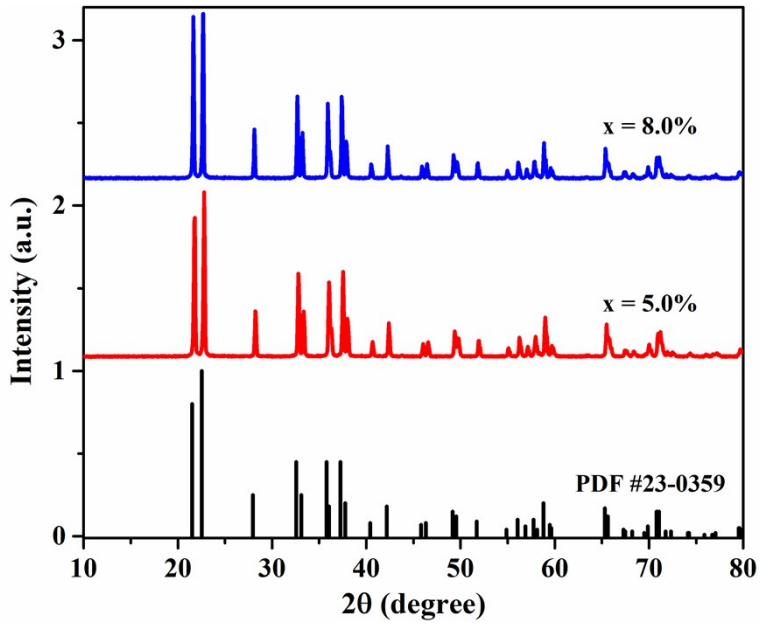

Fig. S11 XRD patterns of $LiGaO_2$:Fe^{3+} sample with high doping concentration.

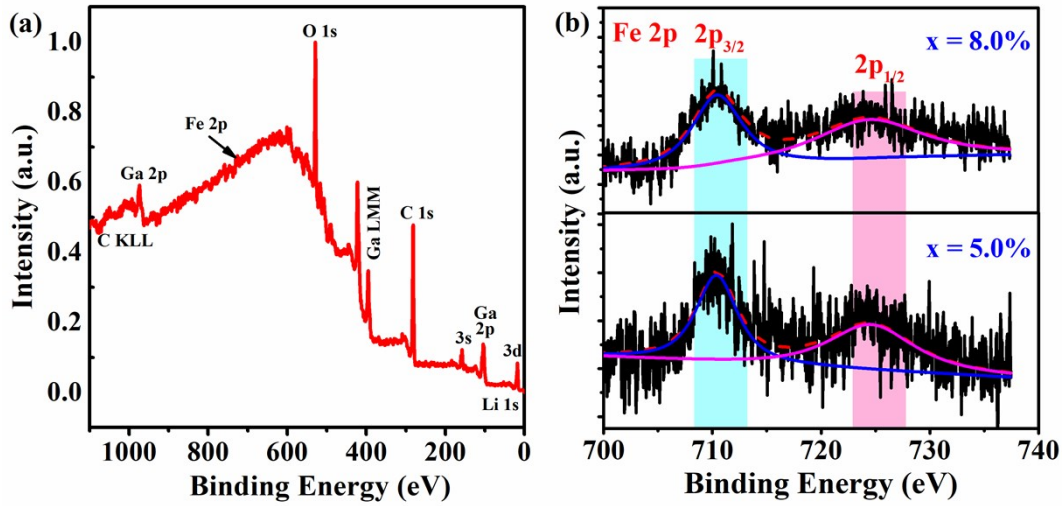

Fig. S12 (a) XPS survey spectrum of $LiGaO_2:Fe^{3+}$ sample. (b) High-resolution XPS spectra of Fe 2p.

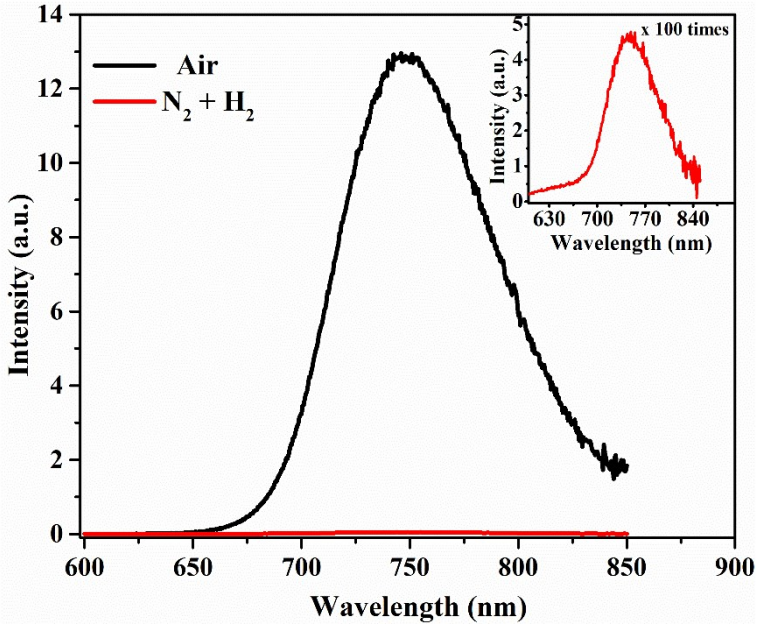

Fig. S13 The PersL spectra for the two isolated $LiGaO_2$:0.25%Fe^{3+} samples using air and reducing atmospheres (95% N_2/5% H_2), respectively. The inset shows the PersL spectrum of the reduced sample (the data was multiplied 100 times).

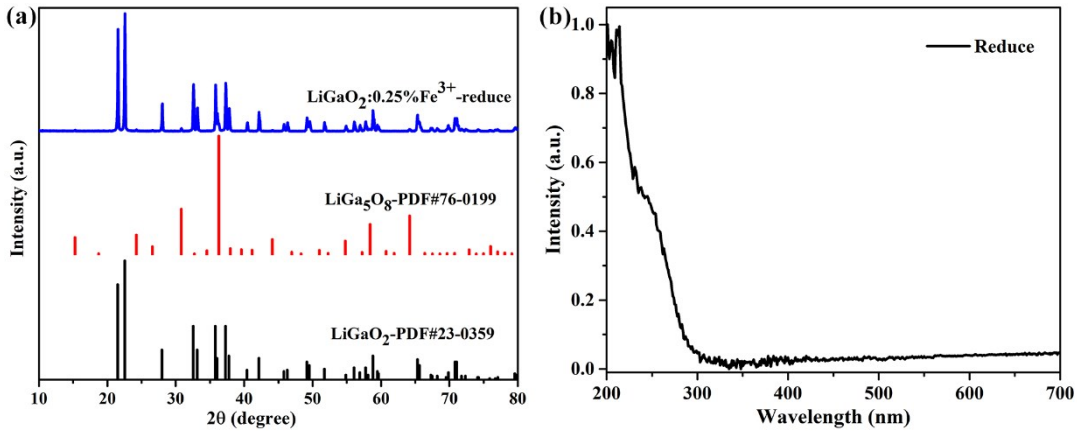

Fig. S14 (a) XRD patterns and (b) Absorption spectrum of the reduced sample.

Under the reducing atmosphere, several diffraction peaks of $LiGa_5O_8$ were generated. Due to the formation of the $LiGa_5O_8$ impurity phase, the NIR PersL performance is greatly weakened, which is consistent with the discussion in Fig. S10 that $LiGa_5O_8$ host is not suitable for the Fe^{3+} to produce NIR PersL.

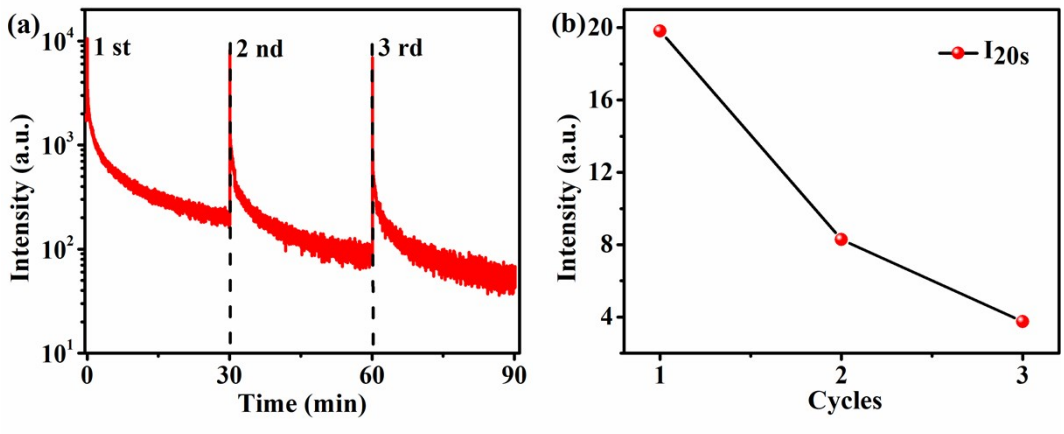

Fig. S15 (a) PersL decay curves of $LiGaO_2$:0.25%Fe^{3+} phosphor upon a household white-light LED illumination for 3 min repeatedly. The sample was first excited by 254 nm UV lamp for 5 min and then put into a dark room waiting for 30 min decay. (b) The PersL decay intensity values at 20 s (I_{20s}) in each cycles.

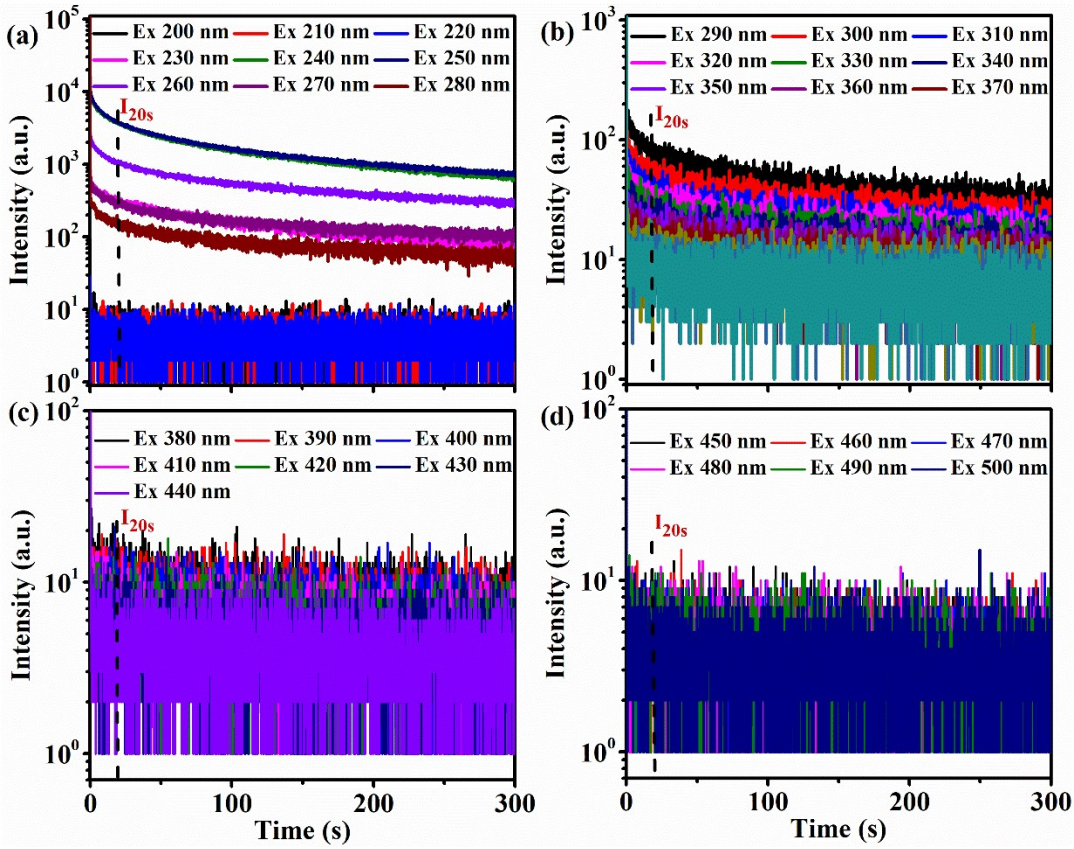

Fig. S16 PersL decay curves of the Fe^{3+}-doped $LiGaO_2$ phosphor excited at various wavelengths (monochromatic light; from the xenon arc lamp in the spectrometer).

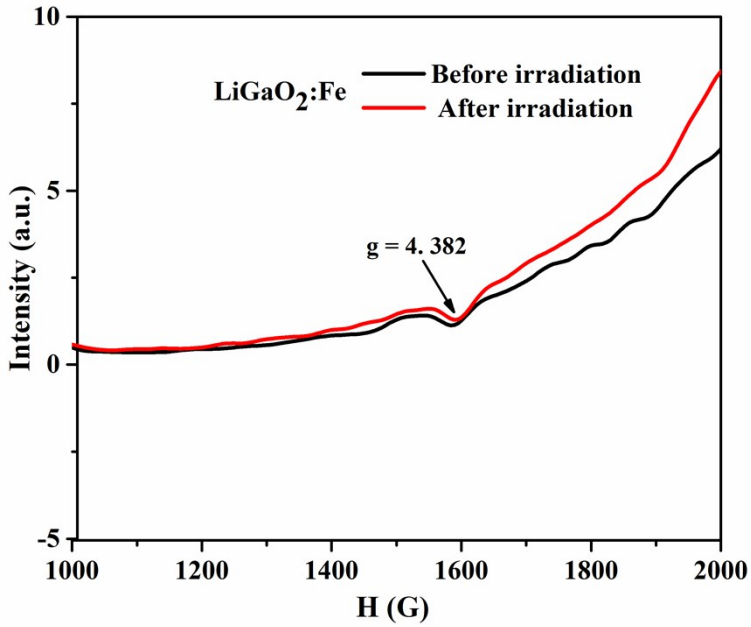

Fig. S17 The enlarge EPR spectrum of the LGO:0.25%Fe^{3+} sample in the range of 1100 to 2100 G.

The signal with g = 4. 382 arises from Fe^{3+} ions in tetrahedral, and it is slightly decreased after irradiation, which originates from the process of Fe-O CT transition (Fe^{3+}-O^{2-} to Fe^{2+}-O^{-}).

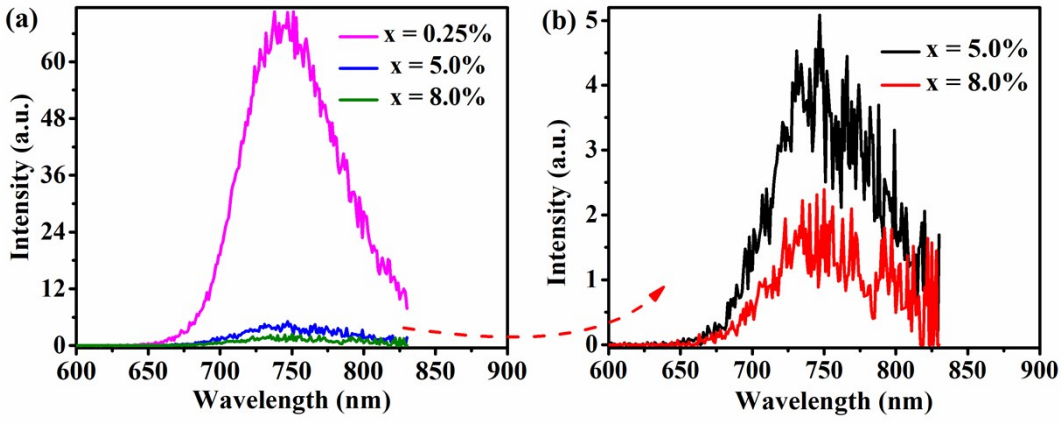

Fig. S18 PersL spectra of $LiGaO_2:Fe^{3+}$ sample with different doping concentration.

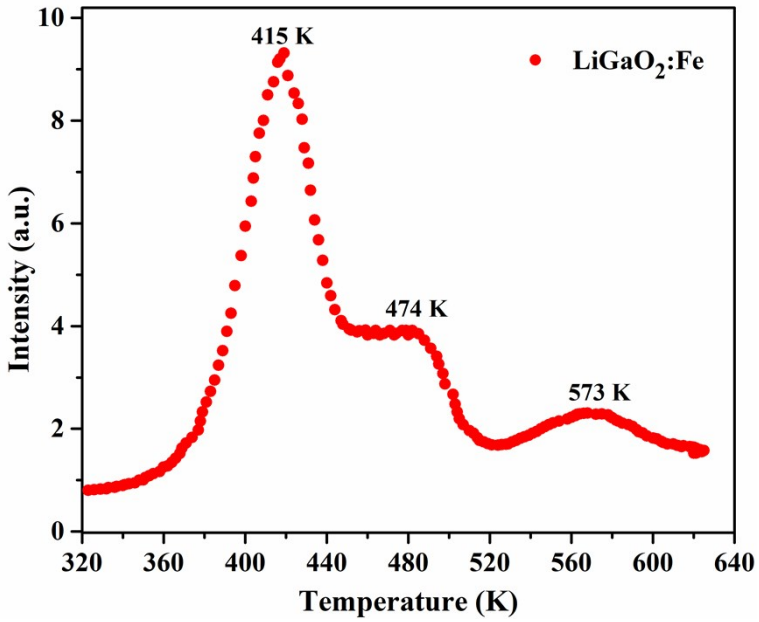

Fig. S19 TL curve of the LGO:0.25%Fe^{3+} sample.

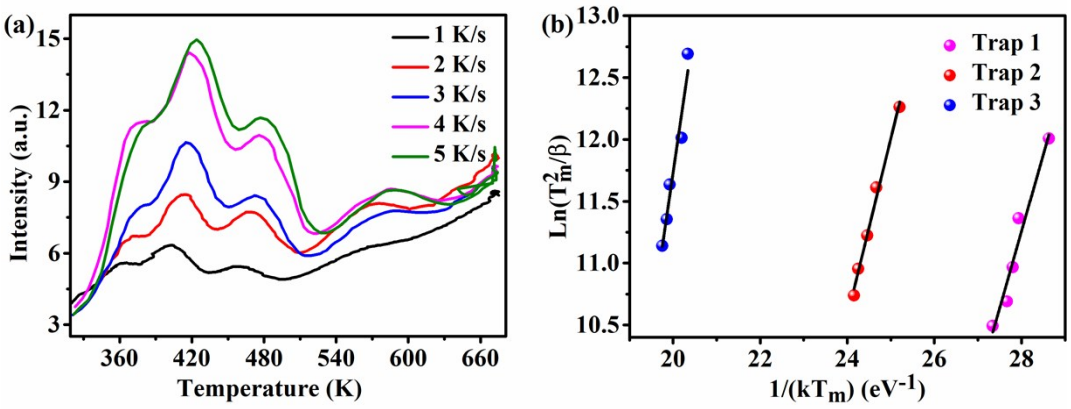

Fig. S20 (a) TL curves of $LiGaO_2$:0.25%Fe^{3+} sample with different heating rate. (b) Trap depths *E* are calculated from the slope of the linear fit by plotting $Ln(T_m^2/\beta)$ *versus* $1/kT_m$.

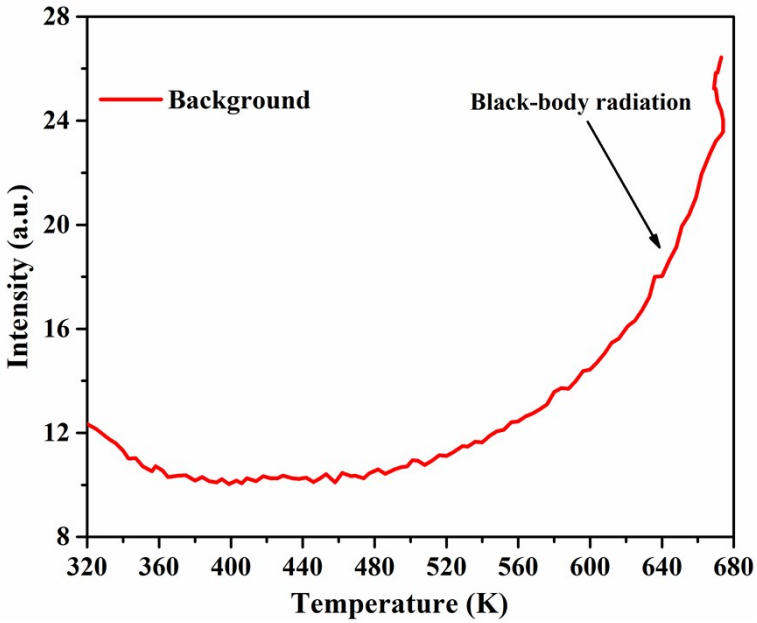

Fig. S21 The effect of black-body radiation on the TL measurement in LGO:Fe NIR PersL material.

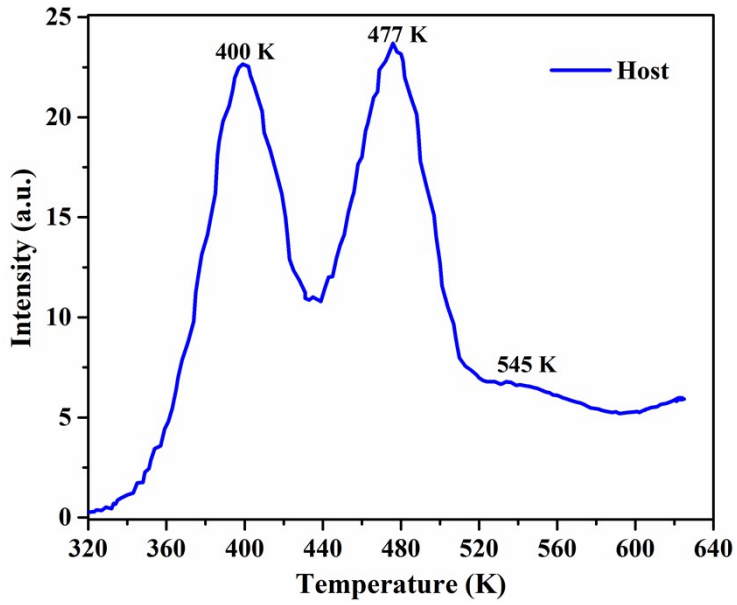

Fig. S22 TL curve of the pure LGO host.

Traces signal of the three TL peaks can be detected, which implies that these traps originate from the intrinsic defects during the high-temperature sintering process. After Fe^{3+} ions incorporated into the LGO host lattice, it should not only increase the trap concentration of Trap 1 but also can accelerate charge carriers stored in Trap 2 transfer to Trap 1.

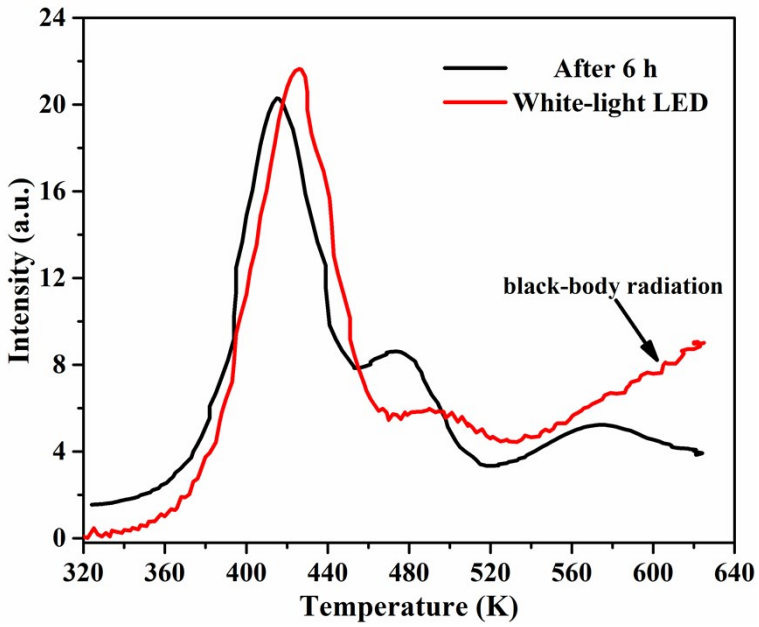

Fig. S23 TL curve of $LiGaO_2$:0.25%Fe^{3+} sample obtained after a decay time of 6 h (black line). The photo-stimulated TL curve after a 6 h decay time was obtained after illuminated for 3 min with white-light LED (red line).

After irradiated with white-light LED, the intensity of Trap 1 slightly increases while the intensity of Trap 2 decreases, which means that the charge carriers stored in Trap 2 are stimulated and gradually release to Trap 1. Therefore, the PersL intensity was recovered when re-irradiated with a white-light LED.

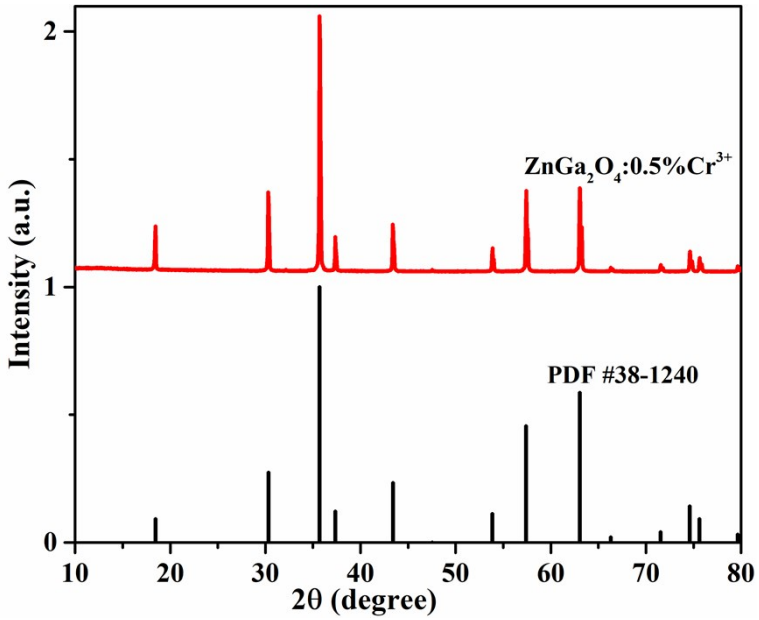

Fig. S24 XRD pattern of $ZnGa_2O_4$:0.5%Cr^{3+} phosphor.

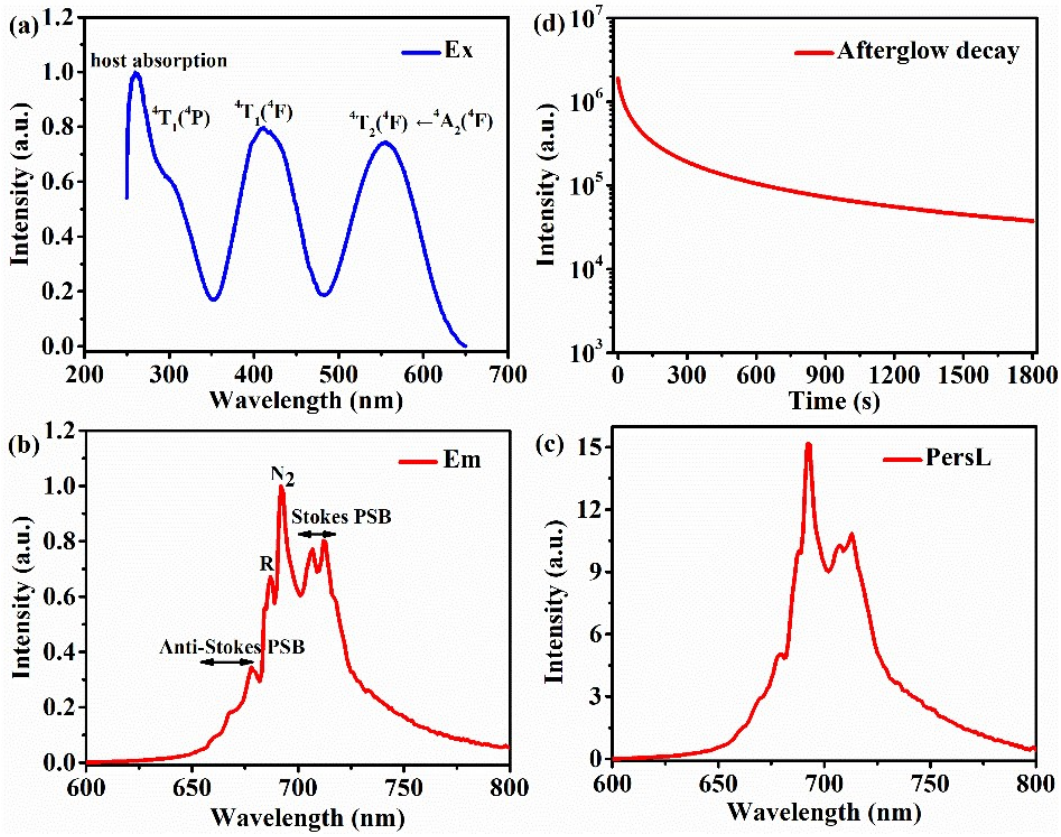

Fig. S25 Optical properties of $ZnGa_2O_4$:0.5%Cr^{3+} phosphor. (a) The normalized PLE spectrum by monitoring the Cr^{3+} emission at 692 nm. (b) The normalized PL spectrum under UV excitation at 262 nm. (c) PersL spectrum recorded at 1 min after the removal of excitation source. (d) PersL decay curve (recorded for 1800 s) by monitoring the Cr^{3+} emission at 692 nm upon UV lamp (254 nm) illumination for 5 min.

References

1. W. Wang, Z. Sun, X. He, Y. Wei, Z. Zou, J. Zhang, Z. Wang, Z. Zhang and Y. Wang, *J. Mater. Chem. C*, 2017, **5**, 4310-4318.

2. K. Kniec, M. Tikhomirov, B. Pozniak, K. Ledwa and L. Marciniak, *Nanomaterials*, 2020, **10**, 189.

3. Z. Zhou, W. Zheng, J. Kong, Y. Liu, P. Huang, S. Zhou, Z. Chen, J. Shi and X. Chen, *Nanoscale*, 2017, **9**, 6846-6853.